2024 46th Annual International Conference of the IEEE Engineering in Medicine and Biology Society (EMBC) | 979-8-3503-7149-9/24/$31.00 ©2024 IEEE | DOI: 10.1109/EMBC53108.2024.10782870

Joint density distributions of dynamic spatial brain networks show systematic variations at rest

Krishna Pusuluri† Armin Iraji† Vince D. Calhoun†
†*Tri-institutional Center for Translational Research in Neuroimaging and Data Science (TReNDS)*
Georgia State University, Georgia Institute of Technology, and Emory University
55 Park Pl NE, Atlanta, GA 30303, USA
Email: kpusuluri1@gsu.edu

***Abstract*—Human resting-state functional magnetic resonance imaging data have been broadly studied previously to identify coherent spatio–temporal patterns of activity in functional brain networks and their dysfunction in brain disorders. While most studies focused on spatially static networks, here we developed an approach to estimate 4D spatially dynamic brain networks, evaluated systematic voxel-wise changes in such networks and the joint density distributions between pairs of networks using two-dimensional (2D) histograms. Clusters of 2D histograms computed using the k-means algorithm across subjects and sliding windows for each network pair showed significant group differences in subject-wise cluster occupancy and dwell time between healthy controls (CN) and patients with schizophrenia (SZ), implying altered network dynamics and interactions. This work provides unique insights into complex network–level relationships and possible dynamical mechanisms underlying SZ, and could potentially help in the development of novel diagnostics and biomarkers.**

***Index Terms*—Resting state fMRI (rsfMRI), dynamic spatial brain networks, schizophrenia, brain disorders, network interactions**

I. Introduction

Several studies on human resting–state functional magnetic resonance imaging (rsfMRI) data investigated coherent spatio–temporal activities of functional brain networks and how such networks got disrupted in disorders such as SZ [1]–[6]. While most earlier studies focused on spatially static regions and looked at their changing relationships over time, recent work focused on spatially dynamic network features and voxel–level interactions within and across networks [3], [7]. Data-driven analytical approaches such as independent component analysis (ICA) have been successfully applied to fMRI data for multivariate source separation, with spatial ICA (sICA) proving helpful to separate fMRI time series data into intrinsic connectivity networks (ICNs) and their associated time courses [1]–[3]. Our recent work [8] presented an approach to identify several spatially dynamic 4D brain networks (with 3D voxels governing a network changing over time) and showed that significant volumetric coupling with synchronized shrinkage and growth existed between pairs of such networks, as well as that several features of these networks were associated with cognition. In addition, SZ affected these networks and resulted in network expansion or shrinkage, altered focus of activity within the networks, reduced spatial dynamic variability within the networks and reduced volumetric coupling between network pairs. As revealed by those findings [8], studying voxel-level changes of dynamic spatial brain networks and their interactions are essential to gain unique insights into the dynamics and mechanisms underlying brain disorders and to develop relevant diagnostic biomarkers. In this study, we present an alternative approach via 2D histograms to study the connectivity and interactions between pairs of dynamic spatial brain networks, their joint density distributions, and disruptions seen in SZ. 2D histograms count the number of occurrences of various combinations of voxel–level intensities/activities and allow for the comparison of two networks. Our results show that joint density distributions of brain network pairs are significantly linked to SZ, with 2D histogram clusters showing either higher or lower cluster occupancy or dwell time in SZ. Our methodology provides global, voxel–agnostic measures to study complex network–level relationships.

This work is funded in part by NIH grants R01MH123610, 5R01MH119251 and NSF grant 2112455. We are grateful to the members of the TReNDS Center for valuable discussions.

II. Methods

We used 3–Tesla rsfMRI data previously obtained in three different studies - The Functional Imaging Biomedical Informatics Research Network (fBIRN) [2], the Center for Biomedical Research Excellence (COBRE) [4], and a Maryland Psychiatric Research Center (MPRC) [5]. Based on the inclusion criteria described in [8], [9], we selected 508 subjects with 315 CN and 193 SZ. Data preprocessing was performed using the statistical parametric mapping toolbox (SPM12, http://www.fil.ion.ucl.ac.uk/spm/) as described in [9], [10]. Fig. 1 depicts the analysis pipeline, starting from group-level spatially constrained independent component analysis (sICA) of rsfMRI data. This is performed with 20 components based on prior research [3], using the group ICA of fMRI toolbox (GIFT) software package [11] (https://trendscenter.org/software/gift/). We identified 14 relevant brain networks or intrinsic component networks (ICNs) and their associated time courses. The mean activity maps for two such networks are shown in Fig. 2. The second step employed prior networks from group-level analysis as a reference to perform spatially constrained ICA across sliding windows for each subject. This was done using multi-objective

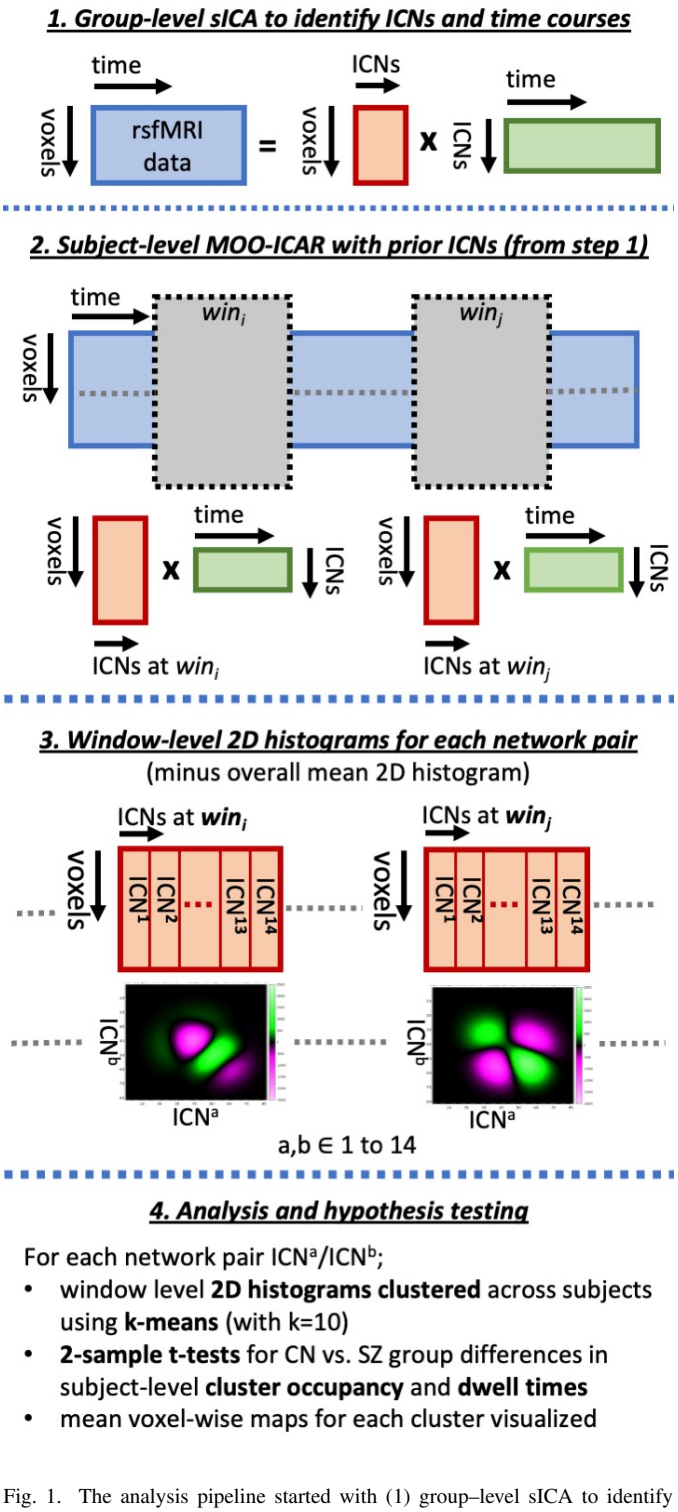

Fig. 1. The analysis pipeline started with (1) group–level sICA to identify intrinsic connectivity networks (ICNs) and their time courses, followed by (2) subject–level multi–objective optimization ICA with reference (MOO–ICAR) over sliding windows that employed prior components (ICNs) from step (1) as reference. For each subject–window and for each brain network pair, 2D histograms were computed (3) and clustered across all the subject–windows using k–means algorithm (after subtracting the overall mean 2D histogram from the window–level data). Further, subject–level cluster occupancies and dwell times were measured and group differences were investigated using 2–sample t–tests and visualizations (4).

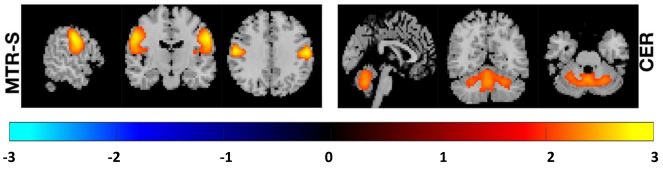

Fig. 2. Mean activity maps (z–scored) across CN group for two example networks: $MTR-S$ (somatomotor secondary) and CER (cerebellar) – shown near the voxel with the highest activity, along three planar cross sections – sagittal, coronal, and transverse. Only regions with $z \geq 2$ are depicted, with anatomical images overlaid in the background.

optimization ICA with reference (MOO-ICAR) [12], [13], integrated in GIFT. This step ensured the correspondence of brain networks across subjects and time windows, and captured the spatial dynamic variability of these networks across windows for each subject. The length of each sliding window is $30 \times TR$ (where the repetition time $TR = 2s$), falling within the recommended range [11]. See [10] for further details on the first two steps of the pipeline. In the third step, 2D histograms were computed at each sliding–window for each subject using z-scored voxel-level activity for a brain network pair. The mean 2D histogram across subjects and windows was computed and subtracted from the window-level 2D histograms in order to focus solely on the changing/differential dynamics, as opposed to overall/mean activity. This was repeated for all 91 possible network pair combinations of 14 brain networks. In the last step, the differential 2D histograms were analyzed further by clustering across subjects and windows using the k-means algorithm (with k=10). For each cluster, two metrics were computed at the subject level – cluster occupancy and cluster dwell time. Cluster occupancy for a given subject and a cluster was defined as the ratio of the number of windows of that subject that fall within the cluster to the total number of windows for the subject. On the other hand, dwell time for a subject and a cluster was defined as the number of consecutive windows on average that fall within the cluster before moving out of the cluster. 2–sample t–tests were performed using subject–level cluster occupancy and dwell time to study CN vs. SZ group differences. We employed a 5% false discovery rate (FDR) [14] correction for multiple comparisons across clusters and network–pairs.

III. Results

Across 20 components used for sICA, we identified 14 relevant brain networks, labeled as $VIS-P$ (visual primary), SUB (subcortical), $MTR-P$ (somatomotor primary), CER (cerebellar), ATN (attention - dorsal), $FRNT$ (frontal), $MTR-S$ (somatomotor secondary), $FPN-R$ (frontoparietal right), $VIS-S$ (visual secondary), $pDMN$ (default mode posterior), $FPN-L$ (frontoparietal left), SN (salience), $TEMP$ (temporal), and $aDMN$ (default mode - anterior) networks. Mean activity maps for two of these networks ($MTR-S$ and CER) are shown in Fig. 2. These networks show voxel-level spatial dynamics, and expand or shrink over

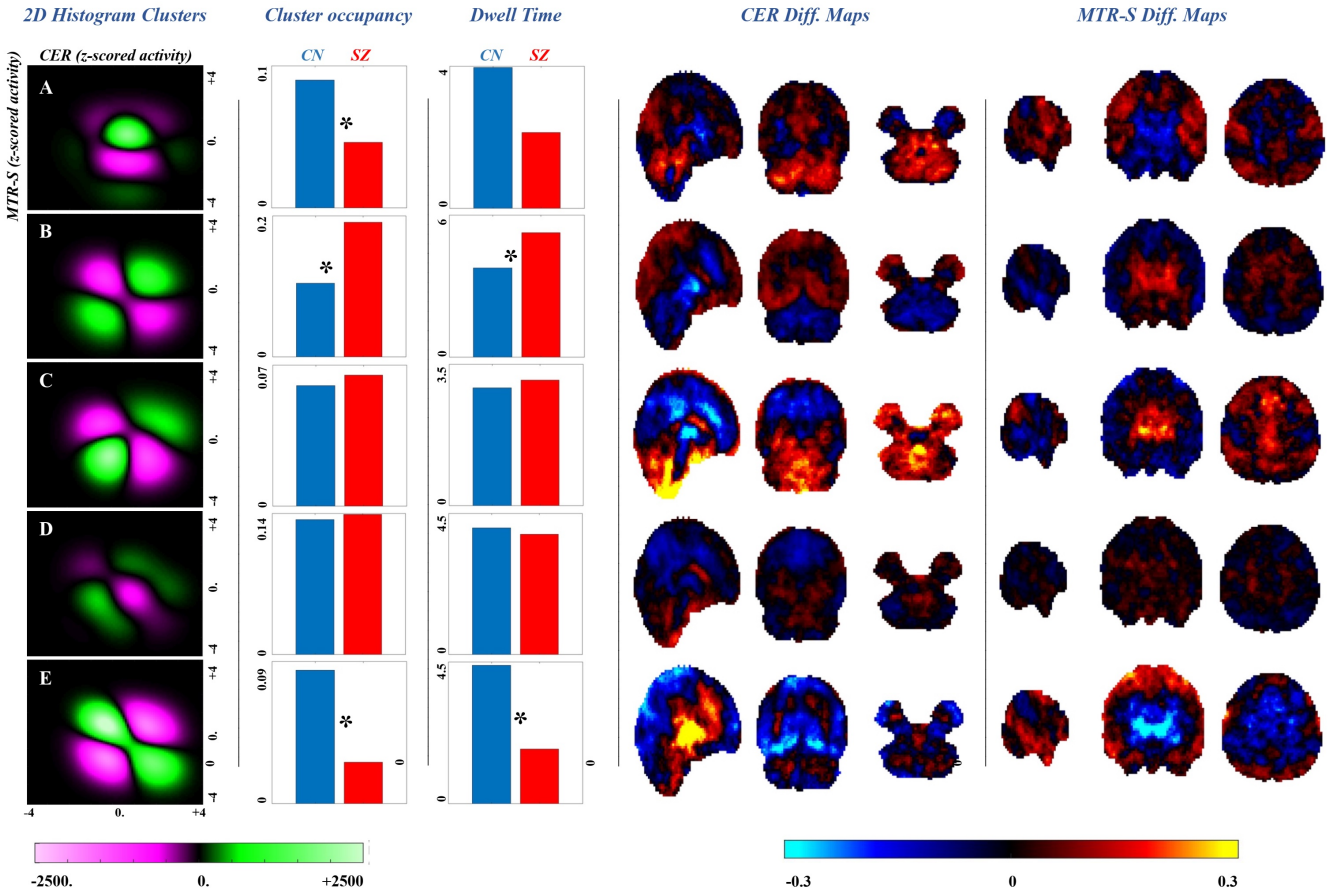

Fig. 3. 2D histogram clusters for joint density distributions, cluster-wise group differences, and mean maps for the network pair CER vs. $MTR-S$ are shown. (A-E) reveal five example k–means clusters (out of k=10) of 2D histograms for the network pair. For each cluster, bar plots show mean cluster occupancies and dwell times for CN and SZ groups (* implies significant group differences). Futhermore, the mean activity maps within each cluster for both the networks are also shown along three orthogonal cross sections (after subtracting the overall network mean map from the cluster mean map). Results reveal dynamical variability and significant group differences across clusters (see also Table. I).

time. See [8] for further details on spatial dynamics of these networks, their coupling, link to cognition, and the effects of Schizophrenia.

For each combination of a pair of networks, 2D histograms were computed at the subject level for each sliding-window and clustered across windows and subjects using k-means algorithm, with $k = 10$. Subject level cluster metrics – cluster occupancy and dwelling time – were measured, and further investigated using 2–sample t–tests for group differences. Table I reveals that several clusters show significant CN vs. SZ group differences in cluster occupancy (purple) and dwell time (green) as revealed by 2–sample t–tests (after 5% FDR correction for multiple comparisons). On the whole, for 91 possible network pairs chosen across 14 brain networks, with 10 k–means clusters per network pair, we find that 291 and 126 of these clusters (out of a maximum of 91*10=910 clusters), respectively, show significant group differences in cluster occupancy and dwell time.

The results for one of these network pairs, CER vs. $MTR-S$, are elaborated further in Fig. 3, which shows five different clusters (out of k=10 clusters, overall) and the corresponding CN vs. SZ bar plots for cluster occupancy and dwell time. Clusters A, B, E show significant group differences in cluster occupancy, while clusters B, D show significant group differences in dwell time, with either higher/lower values possibly seen in SZ compared to CN. The cluster–level mean maps (differential) for both the networks (after subtracting the overall mean maps for the corresponding networks) are also shown, which reveal the network-level dynamic variability across clusters.

IV. Conclusions

We investigated voxel-level changes in dynamic spatial brain networks and their interactions via 2D histograms. This effectively provides a global, voxel–agnostic approach focused on distributional changes among 4D brain networks. We identified 14 relevant brain networks (and 91 possible combinations of network pairs). We employed k–means algorithm (with k=10) to cluster 2D histograms across subjects and sliding–windows. Results showed significant CN vs. SZ group differences in cluster occupancy for 291 clusters and in cluster dwell time for 126 clusters (out of a maximum of 91*10=910

	VIS-P	SUB	MTR-P	CER	ATN	FRNT	MTR-S	FPN-R	VIS-S	pDMN	FPN-L	SN	TEMP	aDMN
VIS-P	0 , 0	3 , 2	3 , 0	8 , 3	7 , 2	6 , 0	5 , 3	4 , 0	5 , 0	5 , 3	4 , 4	4 , 2	5 , 3	5 , 2
SUB	3 , 2	0 , 0	3 , 0	3 , 2	2 , 1	4 , 0	3 , 1	5 , 0	3 , 2	3 , 4	3 , 2	2 , 1	3 , 1	3 , 2
MTR-P	3 , 0	3 , 0	0 , 0	4 , 3	0 , 1	5 , 3	4 , 2	1 , 0	3 , 0	3 , 1	0 , 0	1 , 0	3 , 1	1 , 0
CER	8 , 3	3 , 2	4 , 3	0 , 0	3 , 1	3 , 1	5 , 4	5 , 3	2 , 0	6 , 3	3 , 3	2 , 2	5 , 2	2 , 0
ATN	7 , 2	2 , 1	0 , 1	3 , 1	0 , 0	2 , 1	7 , 5	2 , 1	2 , 0	3 , 2	0 , 0	1 , 0	2 , 1	1 , 0
FRNT	6 , 0	4 , 0	5 , 3	3 , 1	2 , 1	0 , 0	3 , 3	4 , 2	2 , 2	5 , 3	3 , 1	2 , 2	5 , 1	2 , 1
MTR-S	5 , 3	3 , 1	4 , 2	5 , 4	7 , 5	3 , 3	0 , 0	4 , 2	2 , 2	6 , 4	3 , 1	4 , 2	5 , 1	3 , 1
FPN-R	4 , 0	5 , 0	1 , 0	5 , 3	2 , 1	4 , 2	4 , 2	0 , 0	2 , 1	1 , 0	3 , 0	0 , 0	4 , 1	2 , 1
VIS-S	5 , 0	3 , 2	3 , 0	2 , 0	2 , 0	2 , 2	2 , 2	2 , 1	0 , 0	0 , 1	0 , 0	4 , 1	4 , 0	1 , 0
pDMN	5 , 3	3 , 4	3 , 1	6 , 3	3 , 2	5 , 3	6 , 4	1 , 0	0 , 1	0 , 0	2 , 2	3 , 2	4 , 1	2 , 0
FPN-L	4 , 4	3 , 2	0 , 0	3 , 3	0 , 0	3 , 1	3 , 1	3 , 0	0 , 0	2 , 2	0 , 0	2 , 1	7 , 1	1 , 0
SN	4 , 2	2 , 1	1 , 0	2 , 2	1 , 0	2 , 2	4 , 2	0 , 0	4 , 1	3 , 2	2 , 1	0 , 0	5 , 2	4 , 1
TEMP	5 , 3	3 , 1	3 , 1	5 , 2	2 , 1	5 , 1	5 , 1	4 , 1	4 , 0	4 , 1	7 , 1	5 , 2	0 , 0	5 , 3
aDMN	5 , 2	3 , 2	1 , 0	2 , 0	1 , 0	2 , 1	3 , 1	2 , 1	1 , 0	2 , 0	1 , 0	4 , 1	5 , 3	0 , 0

TABLE I

NUMBER OF K-MEANS CLUSTERS (OUT OF K=10) OF 2D HISTOGRAMS FOR EACH NETWORK PAIR WITH SIGNIFICANT CN VS. SZ GROUP DIFFERENCES IN CLUSTER OCCUPANCY (PURPLE) AND DWELL TIME (GREEN) (WITH 5% FDR CORRECTION)

clusters). This work provides unique insights into the dynamics and mechanisms of brain function and dysfunction by studying voxel-level changes within and between brain networks, and their joint density distributions. This could potentially help in the development of novel biomarkers, diagnostics, and pharmacological modulators for SZ in the future.

REFERENCES

[1] Vince D Calhoun, Robyn Miller, Godfrey Pearlson, and Tulay Adalı, "The chronnectome: time-varying connectivity networks as the next frontier in fmri data discovery," *Neuron*, vol. 84, no. 2, pp. 262–274, 2014.

[2] Eswar Damaraju, Elena A Allen, Aysenil Belger, Judith M Ford, S McEwen, DH Mathalon, BA Mueller, GD Pearlson, SG Potkin, A Preda, et al., "Dynamic functional connectivity analysis reveals transient states of dysconnectivity in schizophrenia," *NeuroImage: Clinical*, vol. 5, pp. 298–308, 2014.

[3] Armin Iraji, Thomas P Deramus, Noah Lewis, Maziar Yaesoubi, Julia M Stephen, Erik Erhardt, Aysneil Belger, Judith M Ford, Sarah McEwen, Daniel H Mathalon, et al., "The spatial chronnectome reveals a dynamic interplay between functional segregation and integration," *Human brain mapping*, vol. 40, no. 10, pp. 3058–3077, 2019.

[4] CJ Aine, Henry Jeremy Bockholt, Juan R Bustillo, José M Cañive, Arvind Caprihan, Charles Gasparovic, Faith M Hanlon, Jon M Houck, Rex E Jung, John Lauriello, et al., "Multimodal neuroimaging in schizophrenia: description and dissemination," *Neuroinformatics*, vol. 15, no. 4, pp. 343–364, 2017.

[5] Bhim M Adhikari, L Elliot Hong, Hemalatha Sampath, Joshua Chiappelli, Neda Jahanshad, Paul M Thompson, Laura M Rowland, Vince D Calhoun, Xiaoming Du, Shuo Chen, et al., "Functional network connectivity impairments and core cognitive deficits in schizophrenia," *Human brain mapping*, vol. 40, no. 16, pp. 4593–4605, 2019.

[6] Lorenzo Pini, Charlotte Jacquemot, Annachiara Cagnin, Francesca Meneghello, Carlo Semenza, Dante Mantini, and Antonino Vallesi, "Aberrant brain network connectivity in presymptomatic and manifest huntington's disease: A systematic review," *Human Brain Mapping*, vol. 41, no. 1, pp. 256–269, 2020.

[7] Armin Iraji, Robyn Miller, Tulay Adali, and Vince D Calhoun, "Space: a missing piece of the dynamic puzzle," *Trends in Cognitive Sciences*, vol. 24, no. 2, pp. 135–149, 2020.

[8] Krishna Pusuluri, Zening Fu, Robyn L Miller, Godfrey D Pearlson, Peter Kochunov, Theo GM Van Erp, Armin Iraji, and Vince Calhoun, "4d dynamic spatial brain networks at rest linked to cognition show atypical variability and coupling in schizophrenia, unpublished," *bioRxiv*, pp. 2023–09, 2023.

[9] Armin Iraji, Ashkan Faghiri, Zening Fu, P Kochunov, Bhim M Adhikari, Aysenil Belger, Judith M Ford, S McEwen, Daniel H Mathalon, Godfrey D Pearlson, et al., "Moving beyond the 'cap'of the iceberg: Intrinsic connectivity networks in fmri are continuously engaging and overlapping," *NeuroImage*, vol. 251, pp. 119013, 2022.

[10] Armin Iraji, Jiayu Chen, Noah Lewis, Ashkan Faghiri, Zening Fu, Oktay Agcaoglu, Peter Kochunov, Bhim M Adhikari, Daniel H Mathalon, Godfrey D Pearlson, et al., "Spatial dynamic subspaces encode sex-specific schizophrenia disruptions in transient network overlap and its links to genetic risk," *Biological Psychiatry*, 2023.

[11] Armin Iraji, Ashkan Faghiri, Noah Lewis, Zening Fu, Srinivas Rachakonda, and Vince D Calhoun, "Tools of the trade: estimating time-varying connectivity patterns from fmri data," *Social Cognitive and Affective Neuroscience*, vol. 16, no. 8, pp. 849–874, 2021.

[12] Qiu-Hua Lin, Jingyu Liu, Yong-Rui Zheng, Hualou Liang, and Vince D Calhoun, "Semiblind spatial ica of fmri using spatial constraints," *Human brain mapping*, vol. 31, no. 7, pp. 1076–1088, 2010.

[13] Yuhui Du and Yong Fan, "Group information guided ica for fmri data analysis," *Neuroimage*, vol. 69, pp. 157–197, 2013.

[14] Yoav Benjamini and Daniel Yekutieli, "False discovery rate–adjusted multiple confidence intervals for selected parameters," *Journal of the American Statistical Association*, vol. 100, no. 469, pp. 71–81, 2005.